

An Effective Rapid Electric Vehicle Charger Using a Quasi-Direct Boost - Buck Converter

J. Sreedhar¹, U. Prashanth¹

¹Vignana Bharathi Institute of Technology, Hyderabad, India

Email: sreedharmtech@gmail.com

Abstract

This paper details a quick DC-type battery charger for electric vehicles, with reduced switching losses. A discontinuous PWM (DPWM) control is used, each phase-leg of a typical 3-phase, 2-level voltage source configuration with poor storage of capacitive energy switches off for 240 degrees of the grid essential duration, resulting in just one phase-leg switching every 60 degrees. Therefore, a buck-model DC-DC configuration is used in cascaded connection with the aim of supply current restriction and voltage control for the electric car charging process because the AC-DC network lacks the DC-link voltage controllability. While thinking about charging a Nissan Leaf, we simulated the provided circuit to various options for a built 50 kW battery charger power capability. The data demonstrates that the investigated technology is extremely power efficient.

Keywords. Electric vehicle, charging, battery, boost-buck.

1. INTRODUCTION

The charging market of electric vehicle (EV) is extremely fluid. Companies and organisations engaged in investigation and improvement of in these fields have greatly reduced his charging time for electric vehicles, making it the same as the time users spend charging an internal combustion engine vehicle (ICEV) at a gas station. Currently, most 50kW 400V electric vehicles comply with "CCS - up to 80kW" and "CHAdeMO - around 50kW" fast charging standards Rechargeable. New electric vehicles, alternatively, are built to withstand higher charging powers. As a result, scalability of output power using power electronics building blocks (PEBB) is an important feature of the EV charging system.

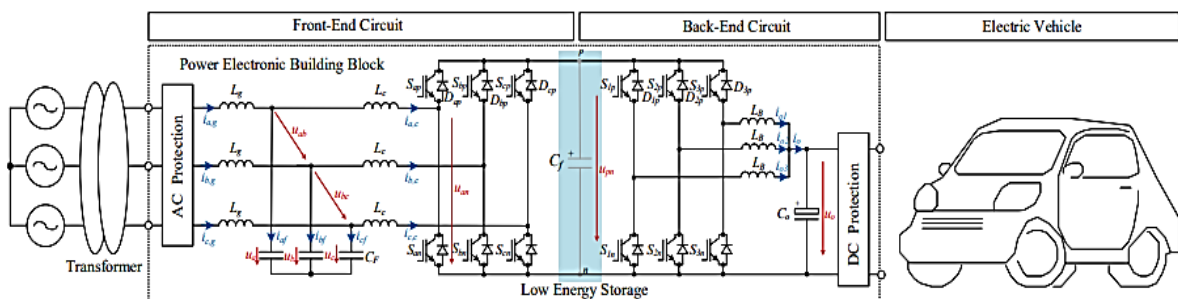
By using a parallel connection, total power can be scaled. This translates into manufacturing benefits because a single circuit package design can be used meet multiple companies and many charging standards. Connecting to the AC grid at medium voltage (MV) levels is becoming economically viable for EV chargers with 100s of kW capacity, as the 380V to 480V grid is most commonly used today.

Proceedings of First International Conference on Smart Systems and Green Energy Technologies (ICSGET 2022)

Where high-capacity chargers are installed, Battery banks and other local energy storage systems can be used to diminish power instabilities and AC grid quality problems. Native renewable power production organisations can also be utilised to reduce power mandate and grid ingesting. In reality, the use of photovoltaic (PV) power generation has great potential. This is because the available area of EV charging station roofs and his buildings in the neighbourhood can exceed 1000 m2. It is also possible to integrate both the battery and the PV array as proposed in [1], into the charger itself.

Figure 1 depicts a bidirectional PEBB configuration suitable for connecting a huge power EV charger using DC type to an MV grid through a 50 Hz transformer. Battery chargers have the advantage of being fully equipped with half-span power modules making them accessible to countless manufacturers with little current rating or interference voltage. A closer look at the circuit in Figure 1 reveals a nice framework of two-stage power conversion. A DC circuit plus a three-stage AC-DC converter A three-channel PWM interleaved DC buck converter is implemented in the circuitry at the rear end. Instead of focusing on similarities with semiconductors, these highlights improved loss sharing between semiconductors or better current distribution amongst the same circuits.

This leads to absolute leadership potential and improved misfortune exchange. Furthermore, the symmetrical PWM interleaving activity compensates for the high repetitive noise compared to the amount of identical circuitry used In the two voltages and flows, the RMS currents in the DC capacitors C_f and C_o are reduced. To accomplish zero-voltage switching of the dynamic switch turn-on and low reverse recovery of the anti-DC diode, this component may be utilised to lengthen the duration waveform in each stage leg of the back-end circuit. Low-complexity and low-cost voltage source rectifier (2L-VSR) with 3-level, 3-wire, 2-level, and 6-level inputs is included into the front-end converter. If the voltage change rate between the AC grid and the EV battery is sufficient, the sustained pressure in the front-end and back-end circuits is enhanced.



Proceedings of First International Conference on Smart Systems and Green Energy Technologies (ICSGET 2022)

Figure 1. Concept of an EV charger with PWM interleaved buck converter for back-end power modification and a 6-switch two-stage bi-directional voltage source rectifier for front-end power modification. It's worth noting that the scaffolds are linked by low-energy DC connections.

This gives the advantage of assembly. In this document, front-end and Back-end circuits are purposefully linked by DC connections using capacitors with low energy storage. Capabilities, such as DC connections without electrolytic capacitors. This deeply couples the activities of the two circuits. The DC connection or voltage between Figure 1 shows a modified encapsulation of the line voltage on an AC capacitor, which essentially corresponds to that achieved by a three-stage diode-span rectifier increase at terminals p and n (or upn). This enables the rectifier stage leg to operate with excellent intermittent PWM balance, allowing the swap to complete within 66 percent or 240° of the grid timeframe. Every 60° , one leg rotates.

This activity was recently revealed in [2], respecting the best exchange fault reduction among all known DPWM schemes, but the voltage of upn It comes at the cost of losing control. The back-end circuitry is critical to the voltage guidelines and current limits of the EV battery charging system. Additionally, if the backend converter is to guarantee consistent power operation, it must provide high power factor operation. He proposed a VIENNA-type front-end circuit in [3], and a DELTA-SWITCH-type front-end circuit with equivalent activity in [4]. The goal of this paper is to examine the benefits of performing DPWN with a 240° terminal switching section on a commonly used 2L-VSR when fast EV battery chargers are used. (e.g., those presented in [5]-[6])

Determining the fundamental characteristics of DC-type EV chargers on the market, appropriate fine-tuning techniques, including fewer replacement accidents, and key control strategies to ensure high-influence factor activity are based on semiconductor and Insightful conditions for determining load impact using passives. Given the converter's AC or DC current amplitude and voltage variation components. The circuit of Figure 1 compares in terms of viable performance [7] with other reasonable answers for a 50kW PEBB frame while considering quick charging of a 30kWh Nissan Leaf vehicle from 0% to 90% state of charge (SoC) will be possible.

2. THREE-PHASE EV BATTERY CHARGER

This section explains how the electric vehicle battery charger shown in Figure 2 works. As previously stated, the front-end Both the front-end and back-end circuits are connected via a DC link with limited energy storage capacity, resulting in highly coupled operation of both circuits. In reality, the circuit is a single-stage three-phase step-down AC-DC converter, with the two highest line-to-line AC voltages switched to the rear output. To regulate the output voltage u_o used for

Proceedings of First International Conference on Smart Systems and Green Energy Technologies (ICSGET 2022)

charging electric vehicles, an end solid-state bridge and cascaded low-pass filtering (LB and Co) are used. Similarly, the output voltage should ideally be adjustable from zero to any value.

$$u_0 < \sqrt{\frac{3}{2}} u_{g,l-l,rms} \quad (1)$$

Note that activity of the back-end circuit applying a (essentially) consistent power P_o prompts a prerequisite of the ongoing I_x fluctuating in stage inverse as a result of the front-end circuit, to the six-beat rectifier voltage. In a 3-wire framework, the sinusoidal state of all AC is maintained for every 60° of mains voltage. mains stage flows $i_{a,b,c}$ is ensured by the superposition of cyclic I_x and current I_y . There is outright pressure in the front-end circuit, which is quickly most reduced.

To exhibit the sinusoidal controllability of the network current, the same circuit displayed in Figure 3 of the framework being scrutinized for lattice separating $[0_o, 30_o]$ or $u_a > u_b > u_c$ (see Figure 3) is considered for examination. Increment. In a perfect world, there is no essential recurrence the voltage drop across the AC inductor causes the EV framework to act as a reasonable three-stage load to the network, with stage conductance G .

$$u_{Lc} = 0 \quad (2)$$

As a result, the value of the controlled current at phase b can be written as

$$\bar{I}_y = -i_{b,c} = -Gu_b \quad (3)$$

$$\bar{u}_y = u_b \quad (4)$$

$$\bar{u}_y = k_y \cdot u_b + (1 - k_y) \cdot u_c = k_y \cdot u_{ac} + k u_c \quad (5)$$

$$k_y = \frac{-u_{pos} - 2u_{neg}}{u_{pos} - u_{neg}} = \frac{u_{bc}}{u_{ac}} \quad (6)$$

$$u_{pos} = \max(u_a, u_b, u_c) \text{ and } u_{neg} = \min(u_a, u_b, u_c) \quad (7)$$

$$\bar{i}_{sbp} = k_y \cdot \bar{I}_y = -k_y \cdot i_{b,c} = -k_y \cdot G \cdot u_b = -G \cdot u_b \cdot \frac{u_{bc}}{u_{ac}} \quad (8)$$

$$i_{a,c} = G \cdot u_a, i_{b,c} = G \cdot u_b \text{ and } i_{c,c} = G \cdot u_c \quad (9)$$

$$\bar{I}_x = k_x \frac{P_o}{u_o} \quad (10)$$

$$k_x = \frac{u_o}{u_{pos} - u_{neg}} \quad (11)$$

$$\bar{I}_x = \frac{P_o}{u_{ac}} = \frac{i_{a,c} \cdot u_{ac} + i_{b,c} \cdot u_{bc}}{u_{ac}} = G \cdot \frac{u_a \cdot u_{ac} + u_b \cdot u_{bc}}{u_{ac}} \quad (12)$$

$$i_{a,c} = \bar{I}_x + \overline{i_{sbp}} = G \cdot u_a \quad (13)$$

$$i_{a,c} + i_{b,c} + i_{c,c} = 0 \text{ and } u_a + u_b + u_c = 0 \quad (14)$$

$$i_{c,c} = \overline{i_{sbm}} - \bar{I}_x = (1 - k_y) \cdot \bar{I}_y - \bar{I}_x = G \cdot u_c \quad (15)$$

$$M_a = \frac{V_{as}}{V_{at}} \quad (16)$$

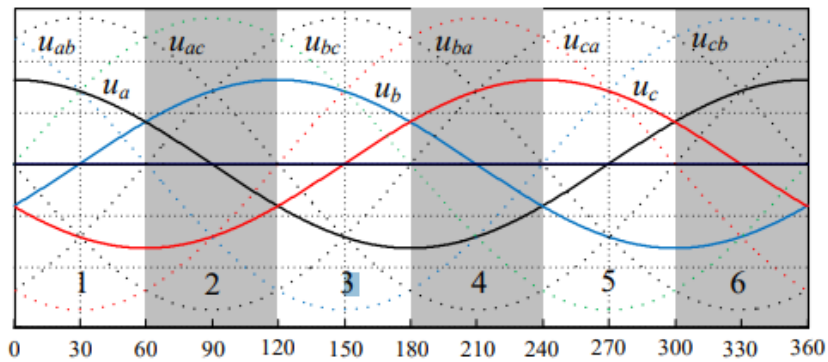


Figure 2. Grid sectors are defined by the various relationships between the instantaneous values of the grid phase voltages u_a, b, c .

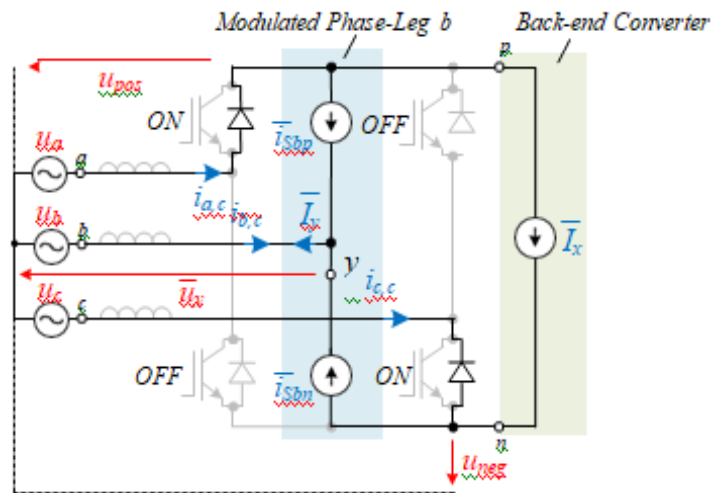


Figure 3. Equivalent circuit of the front-end convert operation for $u_a > u_b > u_c$

$$M_{fr} = \frac{f_{ct}}{f_{rs}} \quad (17)$$

$$v_r > v_c \text{ S11 is on, } V_{out} = \frac{V_d}{2}$$

$$v_r < v_c \text{ S12 is on, } V_{out} = -\frac{V_d}{2}$$

$$m_f = \frac{f_t}{f_m} \quad (18)$$

3. SIMULATION RESULTS

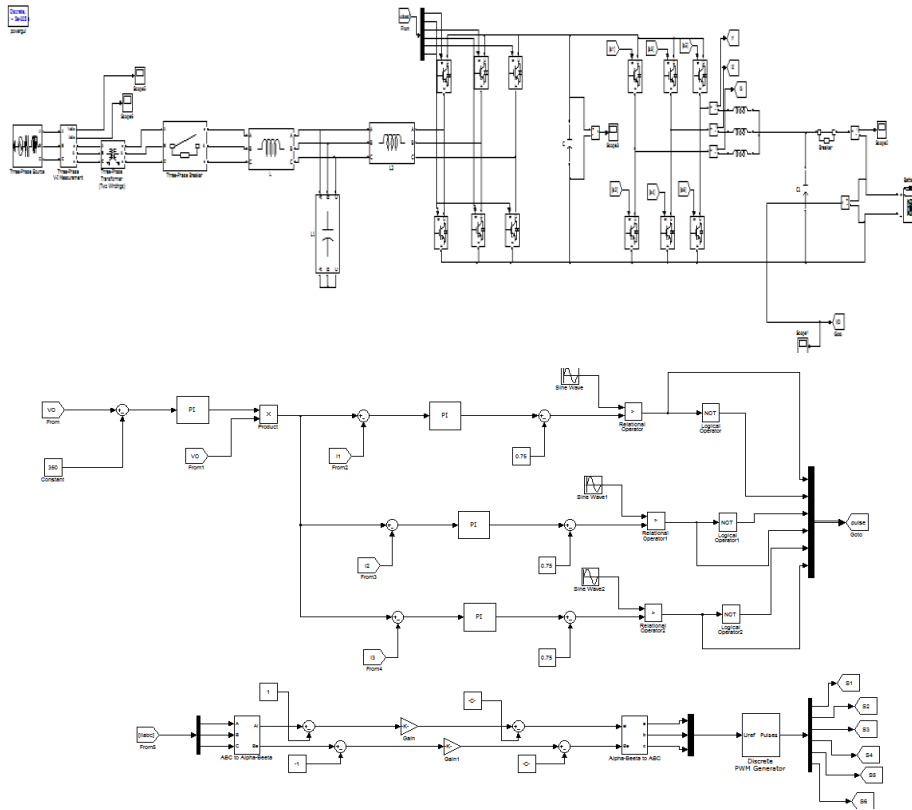


Figure 4. Proposed system circuit configuration

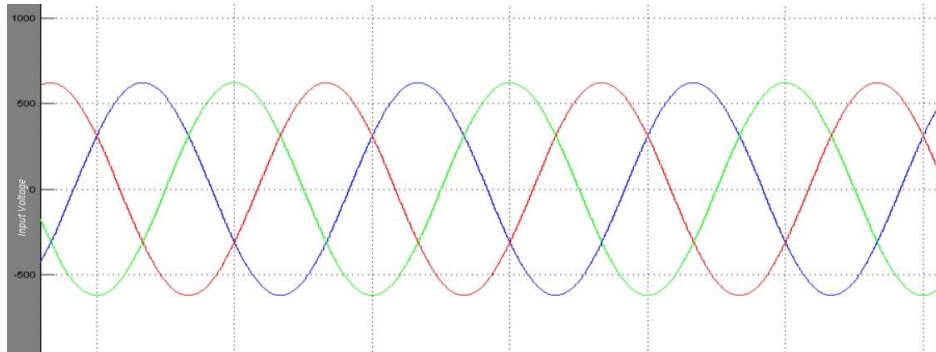


Figure 5. Input voltage for proposed system

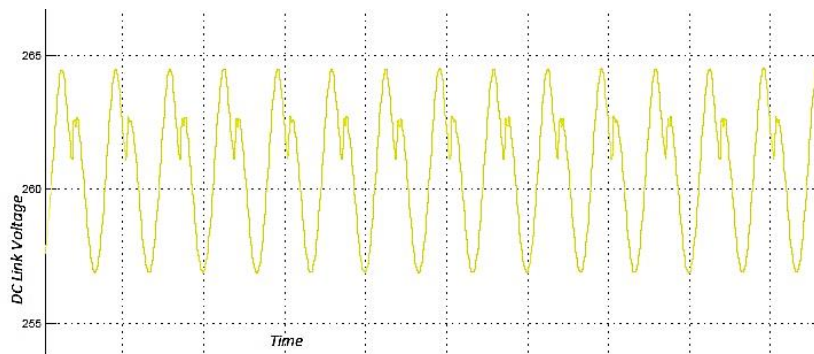
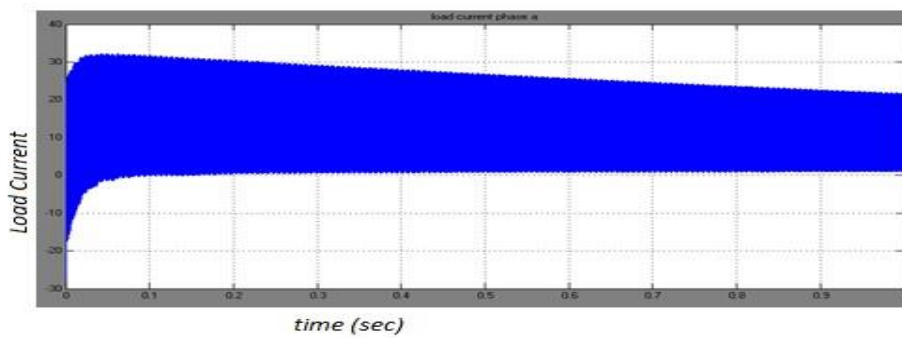
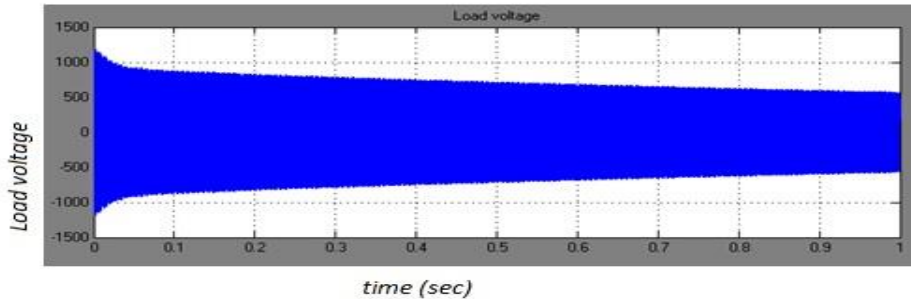


Figure 6. DC-link voltage for proposed system



(a)



(b)

Figure 7. Load voltage and load current

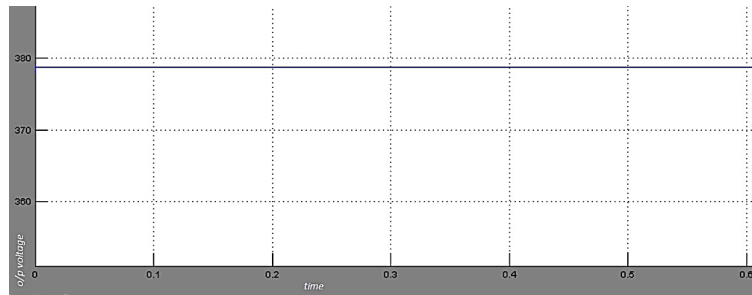


Figure 8. Battery voltage

The findings indicate that the AC flows i_{ac} , i_{bc} , i_{cc} on the converter side can follow the sinusoidal information step voltage u_{abc} , as can be seen very well in Figure 4.6. The same buck converter is running smoothly, so the PEBB-focused circuit and control strategy makes sense. The converter voltage between the step's AC terminal and the DC link's terminal n , confirming that the scaffold leg can complete the exchange for 66 percent of the power grid timeframe increase. The running stresses of scaffold parts, the repetition of appropriate replacements, and the accuracy tests of determined conditions representing the benefits of potential parts were selected. An alternating repetition of $f = 16$ kHz is allocated because it divides well the difference between high productivity, high power density, and high data transmission capacity for control Table II shows the results of the top primaries.

4. CONCLUSION

A three-phase DC battery concept for electric vehicles was studied using a PWM interleaved buck converter for the back end and a two-stage bidirectional voltage source rectifier with six switches for the front end He described his own DPWM modulation implementation. This ensures high power factor operation while also

Proceedings of First International Conference on Smart Systems and Green Energy Technologies (ICSGET 2022)

allowing the phase leg to suspend switching for two-thirds of its line cycle, or 240° resulting in significant switching losses in the semiconductor is reduced to this project covered the working principle, the main design equations, suitable modulation schemes and its PWM control. A benchmark of the semiconductor power consumption figures achieved in his The Nissan Leaf charging session from 0 to 90% was demonstrated. Underneath, a 50kW DC EV charger will be developed using commercially available Wolf Speed SiC MOSFET and Infineon Si IGBT power modules, as well as an appropriate air-cooling system. The analysis also considers the behaviour of grid-tied power conversion using other established modulations, namely SVPWM and DPWM120, as well as his DPWM240 under investigation. The DPWM240 calculations perform admirably in terms of loss reduction and energy savings, as expected.

REFERENCES

- [1] S. Bai and S. M. Lukic, "Unified active filter and energy storage system for an mv electric vehicle charging station," *IEEE Trans. Power Electr.*, 2013.
- [2] J. A. Anderson, M. Haider, D. Bortis, J. W. Kolar, M. Kasper, and G. Deboy, "New Synergetic Control of a 20 kW Isolated Vienna Rectifier Front-End EV Battery Charger," *Proc. of 20th IEEE Workshop on Control and Modeling for Power Electronics (COMPEL)* June 17-20, 2019.
- [3] T. B. Soeiro, and P. Bauer, "Three-phase unidirectional quasi-single- stage delta-switch rectifier + dc-dc buck converter," in *Proc. of 39th Ann. Conf. of the Ind.Electr. Soc., (IECON)*, 2019.
- [4] Ahmet Masum Hava, "Carrier based pwm-vsi drives in the overmodulation region." PhD thesis, 1998.
- [5] M. Hava, R. J. Kerkman, and T. A. Lipo. "A high performance generalized discontinuous pwm algorithm." *IEEE Trans. Ind. Appl.*, pages 1059–1071, 1998.
- [6] L. Schrittwieser, J. W. Kolar and T. B. Soeiro, "99% efficient three- phase buck-type SiC MOSFET PFC rectifier minimizing life cycle cost in DC data centers," in *Proc. Intern. Telecommunications Energy Conference (INTELEC)*, Austin, TX, 2016, pp. 1-8.
- [7] Nagireddy B, sahithipriya. Kosika, manishpatel. Gadam, jagadhishwar. Banoth, ashok. Banoth, Srikanth goud. B, "Analysis of positive output buck-boost topology with extended conversion ratio", *Journal of Energy Systems*, 6(1), pp. 62–83, 2022.